Insight — Application Note 2.17

Electrical Modeling of Polymers

Introduction

The dielectric—literally "two-electric"—properties of conductivity σ, and permittivity ε, arise from ionic current and dipole rotation in bulk material. For polymers, mobile ions are often due to impurities and additives, while dipoles result from the separation of charge on nonpolar bonds or across a molecule. When analyzing dielectric properties, it is possible and convenient to separate the influence of ions from dipoles, as shown in Figure 17-1.a., to consider their individual effects.

Ions and Dipoles

The flow of ions in an electric field is called current, and is determined by conductivity σ, or its inverse resistivity ρ. The bulk effect of mobile ions can be modeled as a conductance G, as shown in Figure 17-1.b. This conductance changes as ion mobility changes. In turn, mobility depends on the state of a material—its viscosity when liquid or its modulus when solid. As a result, electrical measurements can be a means of probing material state.

The mechanical property of fluid viscosity impedes ionic motion, leading to the term *ion viscosity* to describe the electrical property of resistivity ρ. More specifically, *ion viscosity* should be reserved to describe the frequency independent resistivity ρ_{DC}. During the cure of thermosetting resin systems, comparisons of mechanical viscosity and ion viscosity have demonstrated that often the two differ by only an offset and a scaling factor. Thus ion viscosity can provide valuable insight into the condition of a polymer during processing. Furthermore, measurable changes in ion viscosity occur up to the end of cure—past the time when mechanical viscosity can no longer be measured.

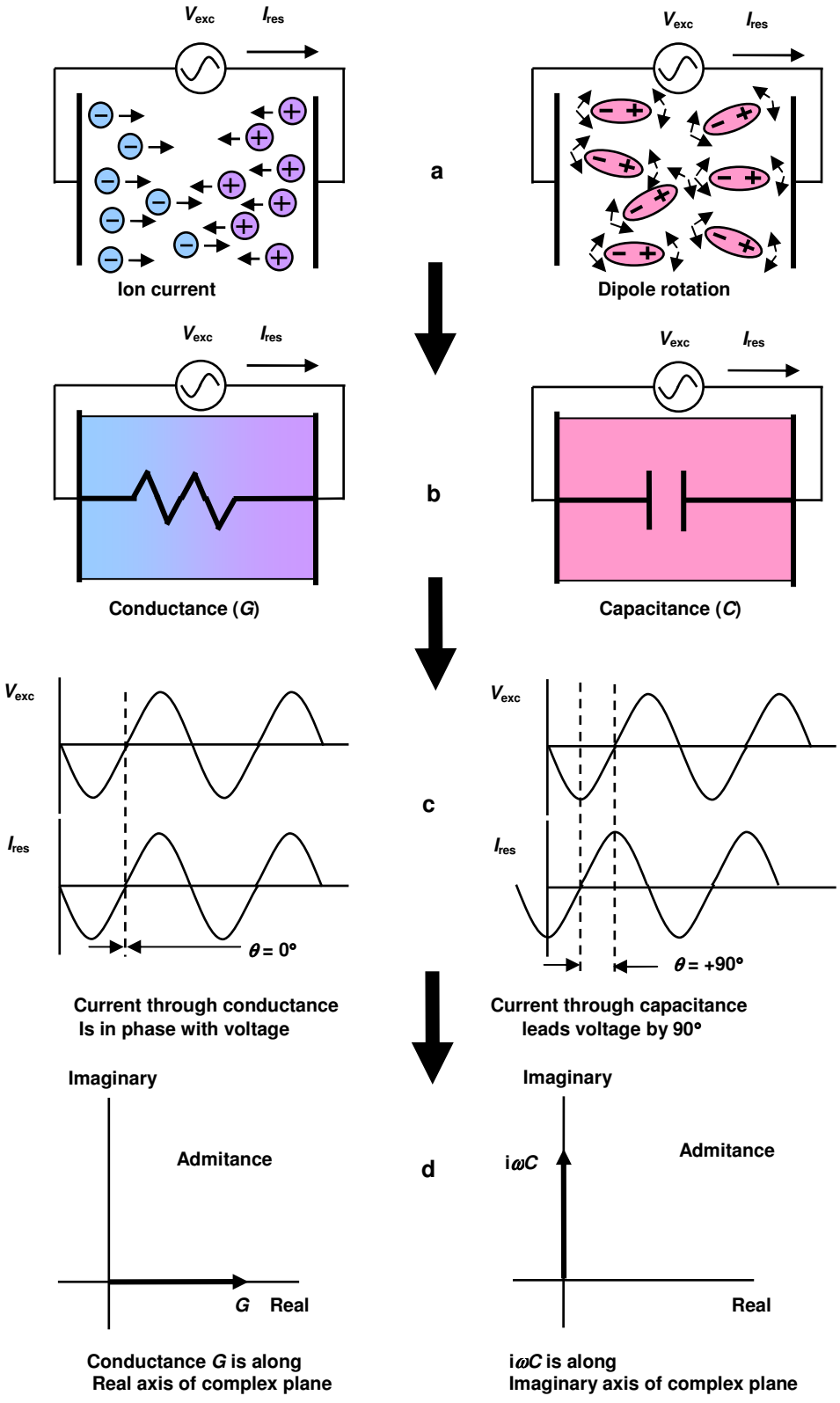

Figure 17-1
Relationships between physical and electrical behavior

The current through a conductance is in phase with the voltage across it, as shown in Figure 17-1.c. Admittance Y is given by equations 17-1 and 17-2:

(eq. 17-1) $Y = I/V$

(eq. 17-2) $Y = G + i\omega C$

Where: I = current (A)
V = voltage (V)
G = conductance (moh)
C = capacitance (F)
ω = $2\pi f$ (s^{-1})
f = frequency (Hz)

Current I and voltage V in general are complex quantities. An admittance consisting only of conductance G can be represented as a vector along the Real axis in the complex plane, as shown in Figure 17-1.d.

The rotation of dipoles is a second material phenomenon, as shown in Figure 17-1.a, and gives rise to permittivity ε. As dipoles change their orientation in response to an electric field, they store energy which is released when their orientation returns to the relaxed state. This energy storage can be modeled as a capacitor, as shown in Figure 17-1.b.

The sinusoidal current through a capacitance leads the voltage across it by 90° as shown in Figure 17-1.c. An admittance consisting only of ωC can be portrayed on the complex plane as a vector along the Imaginary axis, as shown in Figure 17-1.d.

Raw dielectric measurements are conductance G (mohs) and capacitance C (farads). Resistance and other material properties are given by equations 17-3 through 17-7:

(eq. 17-3) $R = 1/G$ (resistance)

(eq. 17-4) $\rho = R\,A/D$ (resistivity or ion viscosity)

(eq. 17-5) $\sigma = G / (A/D)$ (conductivity)

(eq. 17-6) $\varepsilon' = C / (\varepsilon_o\, A/D)$ (relative permittivity)

(eq. 17-7) $\varepsilon'' = \sigma / (\varepsilon_o\, \omega)$ (loss factor)

Where: ε_0 = 8.85×10^{-14} F/cm (permittivity of free space)
A/D = ratio of area to distance for electrodes

Although *A*/*D* is classically applied to parallel plate geometries, it may be generalized to other configurations as a scaling factor, or cell constant, which makes equations 17-4, 17-5 and 17-6 true. In this case, *A* is not necessarily the area of the electrodes and *D* is not necessarily the distance between them. Two dimensional numerical simulations of electrodes in lossy media have validated this generalization across a wide range of conductivity.

The combined quantities *G* and *C* may be visualized on the complex plane as shown in Figure 17-2, where *G* is the real component of the admittance and ωC is the imaginary component. After bulk quantities *G* and *C* are divided by *A*/*D* and ε_0, the material properties of σ/ε_0 and relative permittivity ε' remain, resulting in rescaled values on the complex plane.

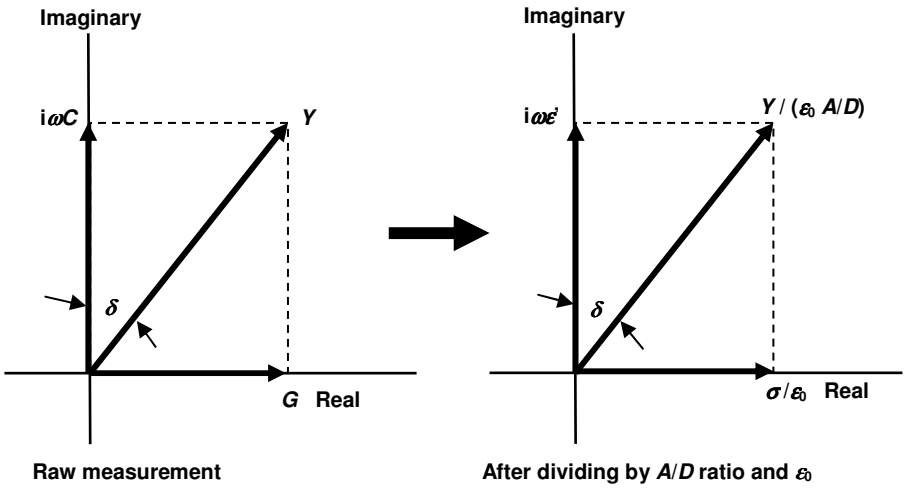

Figure 17-2
Relationship between bulk and material properties

The angle δ between *Y* and the imaginary axis may be incorporated into a quantity called dissipation factor, or loss tangent, tan δ, given by equation 17-8:

(eq. 17-8) $$\tan \delta = \sigma/(\omega \varepsilon_0 \varepsilon')$$

Use of loss factor in equation 17-8 yields the more common expression for loss tangent:

(eq. 17-9) $$\tan \delta = \varepsilon''/\varepsilon'$$

If a material has low conductivity or the frequency is very high, then ε'' and the ratio $\varepsilon''/\varepsilon'$ are small. In this case tan $\delta \sim \delta$ and δ may be approximated by equation 17-10:

(eq. 17-10) $$\delta \sim \varepsilon''/\varepsilon'$$

Electrical model of Material Under Test (MUT)

Dielectric measurements of a Material Under Test (MUT) yield a bulk conductance G_{MUT} in parallel with a bulk capacitance C_{MUT}, which can be used in the electrical model of Figure 17-3. In general, both components have frequency dependent and frequency independent terms. Similarly, the material properties of conductivity σ and permittivity ε have frequency dependent and independent behavior.

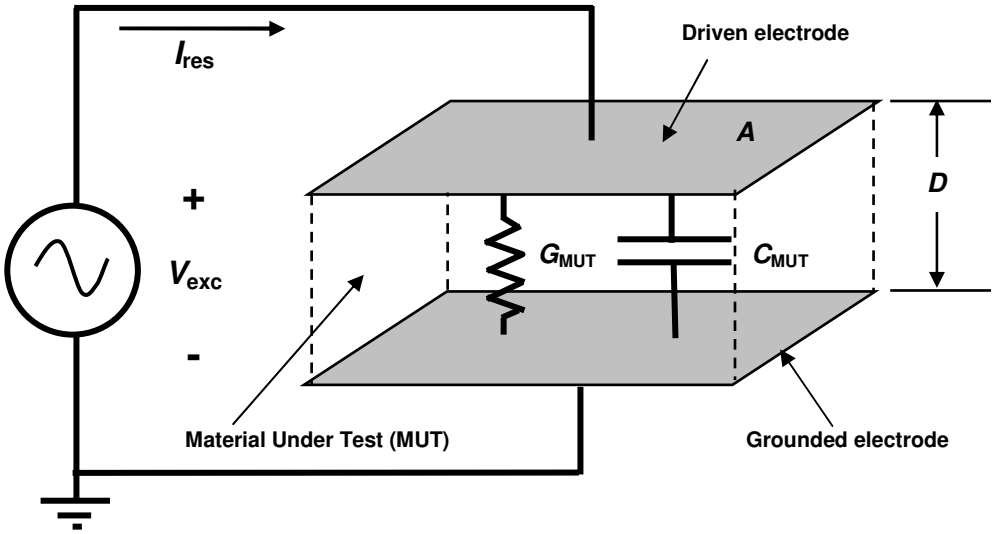

Figure 17-3
Electrical model of a polymer

It is easier to understand the electrical behavior of a polymer by considering Figure 17-4, which uses circuit components corresponding to the following physical phenomena:

- Flow of ions
    - Ion current in an electric field is determined by mobility in the polymer network
    - Current is frequency independent to first order in common polymers
    - Modeled by conductance G_{ion}
- Rotation of induced dipoles
    - Induced dipoles result from charge separation on nonpolar bonds
    - Induced dipoles rotate in an electric field without energy loss
    - Rotation has a frequency independent response
    - Modeled by capacitance $C_{induced}$
- Rotation of static dipoles
    - Static dipoles result from charge separation on molecules
    - Static dipoles rotate in an electric field with energy loss from friction
    - Rotation has a frequency dependent response with relaxation time τ
    - Modeled by conductance G_{static} in series with capacitance C_{static}

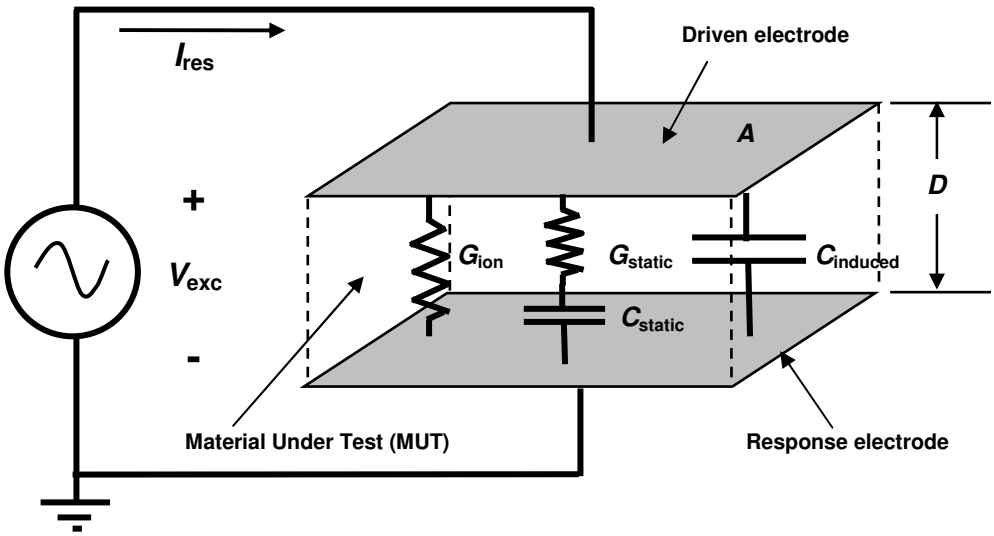

Figure 17-4
Electrical model of polymer physical behavior

It is possible to interpret the model of Figure 17-4 in terms of the measured quantities of conductance G_{MUT} and C_{MUT}. From circuit theory, the admittance of Figure 17-4 is given by equation 17-11:

(eq. 17-11) $$Y_{MUT} = G_{ion} + i\omega C_{induced} + i\omega C_{static} /(1 + i\omega\tau)$$

Where: $\tau = R_{static} C_{static}$ (dipole relaxation time)
$R_{static} = 1/G_{static}$

Admittance can be expressed by keeping real and imaginary terms together:

(eq. 17-12) $$Y_{MUT} = [G_{ion} + \omega^2\tau C_{static}/(1 + (\omega\tau)^2)] + i\omega[C_{induced} + C_{static}/(1 + (\omega\tau)^2)]$$

Combining equations 17-2 and 17-12 yields the following expressions for the measured bulk quantities:

(eq. 17-13) $$G_{MUT} = G_{ion} + C_{static} [\omega^2 \tau /(1 + (\omega\tau)^2)]$$

(eq. 17-14) $$C_{MUT} = C_{induced} + C_{static}/(1 + (\omega\tau)^2)$$

Combining equations 17-5, 17-6, 17-7 and 17-13 results in the expressions for conductivity, loss factor and relative dielectric constant:

(eq. 17-15) $$\sigma_{MUT} = \sigma_{ion} + \varepsilon_{static} [\omega^2 \tau /(1 + (\omega\tau)^2)]$$

(eq. 17-16) $$\varepsilon''_{MUT} = \sigma_{ion}/(\omega\varepsilon_0) + [\varepsilon_{static} /\varepsilon_0][\omega \tau /(1 + (\omega\tau)^2)]$$

(eq. 17-17) $$\varepsilon'_{MUT} = (\varepsilon_{induced} /\varepsilon_0) + (\varepsilon_{static} /\varepsilon_0) /(1 + (\omega\tau)^2)$$

At low frequencies the *relaxed relative permittivity* is the sum of dielectric constants due to both static and induced dipoles. At high frequencies the *unrelaxed relative permittivity* is due only to induced dipoles. They are defined as follows:

(eq. 17-18) $$\varepsilon'_r = (\varepsilon_{static} + \varepsilon_{induced})/\varepsilon_0$$ (relaxed relative permittivity)

(eq. 17-19) $$\varepsilon'_u = \varepsilon_{induced} /\varepsilon_0$$ (unrelaxed relative permittivity)

The relative dielectric constant resulting from static dipoles may be expressed in terms of the relaxed and unrelaxed relative dielectric constants by using equations 17-18 and 17-19:

(eq. 17-20) $$\varepsilon_{static}/\varepsilon_0 = \varepsilon'_r - \varepsilon'_u$$

Combining equations 17-16, 17-17, 17-19 and 17-20 yields equations for the dielectric response:

(eq. 17-21) $$\varepsilon''_{MUT} = \sigma_{ion}/\omega\varepsilon_0 + (\varepsilon'_r - \varepsilon'_u)\frac{\omega\tau}{1 + (\omega\tau)^2}$$

(eq. 17-22) $$\varepsilon'_{MUT} = \varepsilon'_u + \frac{\varepsilon'_r - \varepsilon'_u}{1 + (\omega\tau)^2}$$

Where: ε'_u = Unrelaxed (high frequency) relative permittivity
ε'_r = Relaxed (low frequency) relative permittivity
$\omega = 2\pi f$ (radians/s)
$\tau = R_{static}\, C_{static}$ (s)

Debye equations for dipolar rotation

Neglecting the ionic conductivity term, equations 17-21 and 17-22 also happen to be the loss factor and permittivity as expressed by the Debye equations, which describe the behavior of rotating dipoles. General admittance *Y* is given by equation 17-2, presented earlier:

(eq. 17-2) $$Y = G + i\omega C$$

Equation 17-2 may be rearranged to define admittance as a complex admittance $i\omega C^*$:

(eq. 17-23) $$i\omega C^* = i\omega(C - iG/\omega)$$

Dividing both sides of equation 17-23 by $i\omega\varepsilon_0$ and the *A*/*D* ratio yields a complex permittivity ε^*:

(eq. 17-24) $$\varepsilon^* = \varepsilon' - i(\sigma/\varepsilon_0\omega)$$

Finally, from the definition of loss factor (eq. 17-7), the complex permittivity may be expressed as follows:

(eq. 17-25) $$\varepsilon^* = \varepsilon' - i\varepsilon''$$

The classic Debye equation for dielectric relaxation, as a complex number and function of frequency, is:

(eq. 17-26) $$\varepsilon^*(\omega) = \varepsilon'_u + \frac{\varepsilon'_r - \varepsilon'_u}{1 + i\omega\tau}$$

Where: ε'_u = Unrelaxed (high frequency) relative permittivity
ε'_r = Relaxed (low frequency) relative permittivity
$\omega = 2\pi f$ (radians/s)
τ = Dipole relaxation time (s)

Separating real and imaginary components of equation 17-26 yields the Debye equations for loss factor and relative permittivity:

(eq. 17-27) $$\varepsilon'' = \mathrm{Im}(\varepsilon^*(\omega)) = \frac{(\varepsilon'_r - \varepsilon'_u)\,\omega\tau}{1 + (\omega\tau)^2}$$

(eq. 17-28) $$\varepsilon' = \mathrm{Re}(\varepsilon^*(\omega)) = \varepsilon'_u + \frac{\varepsilon'_r - \varepsilon'_u}{1 + (\omega\tau)^2}$$

Loss factor ε'' and relative permittivity ε' are plotted as a function of $\omega\tau$ in Figure 17-5. The loss peak and the inflection point of relative permittivity both occur at $\omega\tau = 1$.

A common diagram is the Cole-Cole plot shown in Figure 17-6. When loss factor is plotted vs. permittivity, the Debye equations form a semi-circle. This ideal behavior results from the assumption of a single dipolar time constant τ. In reality, a single relaxation time does not account for the effect of molecular weight distributions, varying locations along a polymer chain or the environment

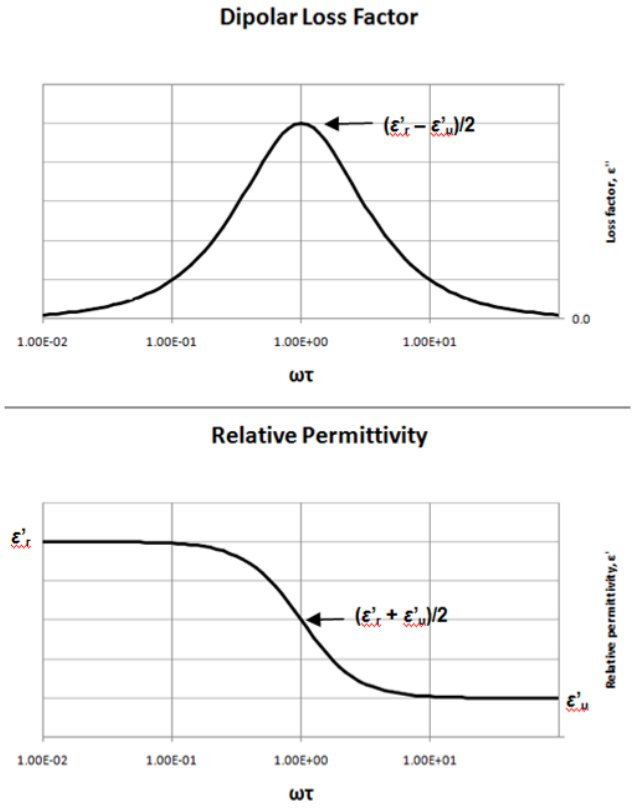

Figure 17-5
Debye relaxation behavior for loss factor and relative permittivity

.

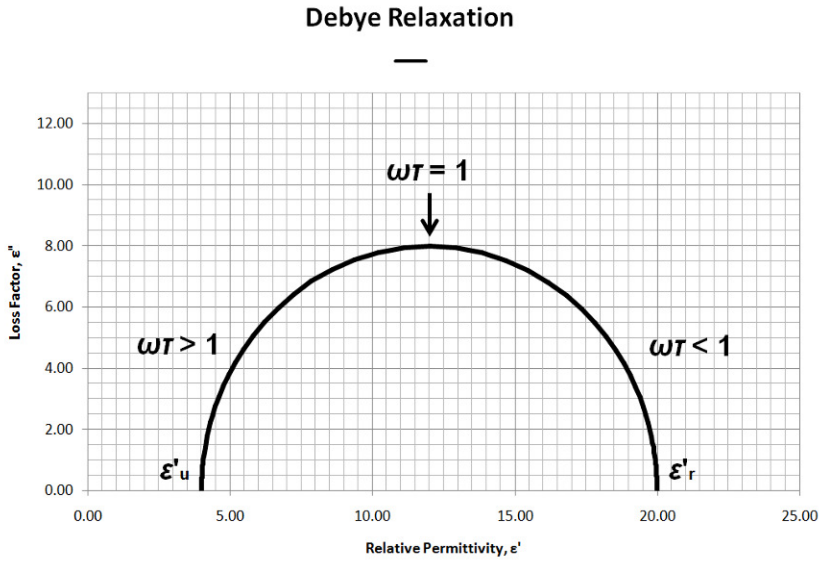

Figure 17-6
Cole-Cole plot of Debye relaxation

Variants of the Debye equations

In polymers and thermosets, it is common to find non-ideal dipole relaxation behavior, resulting in Cole-Cole plots that are squashed compared to the semi-circle of the Debye equations. This response has been attributed to the superposition of a range of relaxation times. The Cole-Cole plot may also be asymmetric, supposedly corresponding to asymmetric distributions of relaxation times.

Three common variants of the Debye equations attempt to empirically model non-ideal dipole behavior:

- Cole-Cole relaxation[1,2] (squashed plots)

(eq. 17-29)
$$\varepsilon^*(\omega) = \varepsilon'_u + \frac{\varepsilon'_r - \varepsilon'_u}{1 + (i\omega\tau)^{1-\alpha}} \qquad (0 \le \alpha \le 1)$$

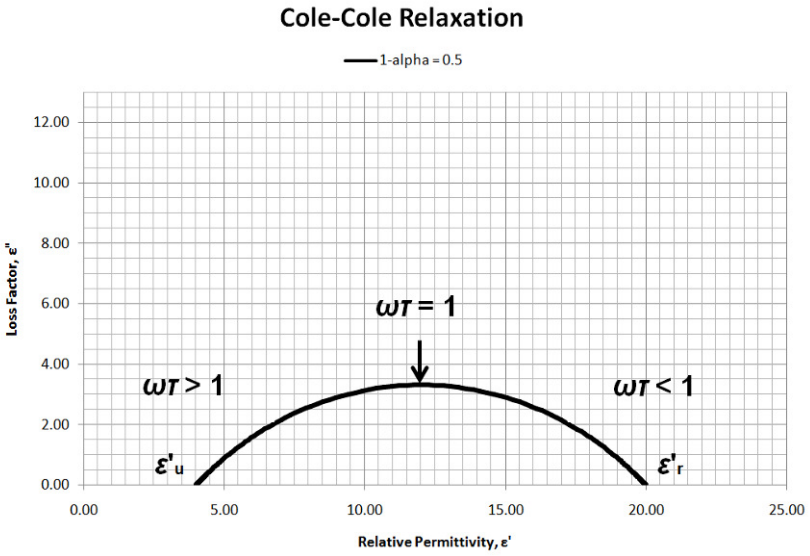

Figure 17-7
Cole-Cole plot of Cole-Cole relaxation

- Cole-Davidson[3] relaxation (asymmetric plots)

(eq. 17-30)
$$\varepsilon^*(\omega) = \varepsilon'_u + \frac{\varepsilon'_r - \varepsilon'_u}{(1 + i\omega\tau)^{\beta}} \qquad (0 \le \beta \le 1)$$

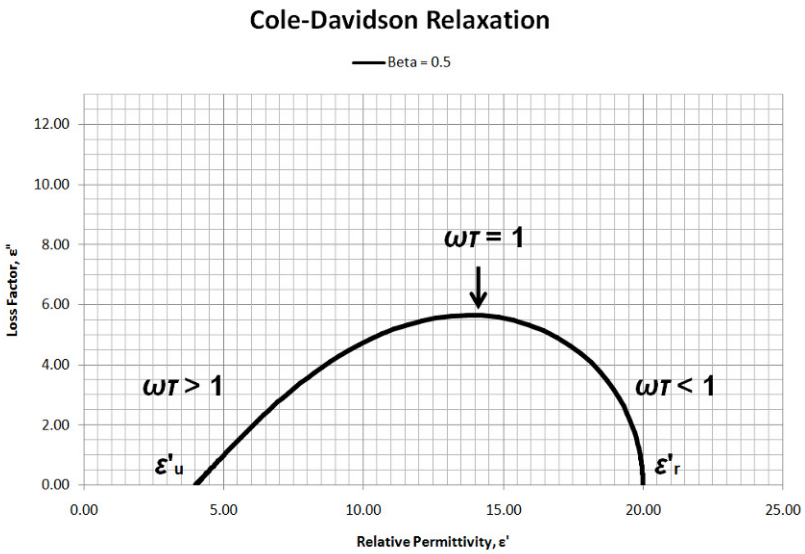

Figure 17-8
Cole-Cole plot of Cole-Davidson relaxation

- Havriliak-Negami relaxation[4] (squashed and asymmetric plots)

(eq. 17-31)
$$\varepsilon^*(\omega) = \varepsilon'_u + \frac{\varepsilon'_r - \varepsilon'_u}{(1 + (i\omega\tau)^{\alpha})^{\beta}} \qquad \begin{matrix}(0 \le \alpha \le 1) \\ \text{and} \\ (0 \le \beta \le 1)\end{matrix}$$

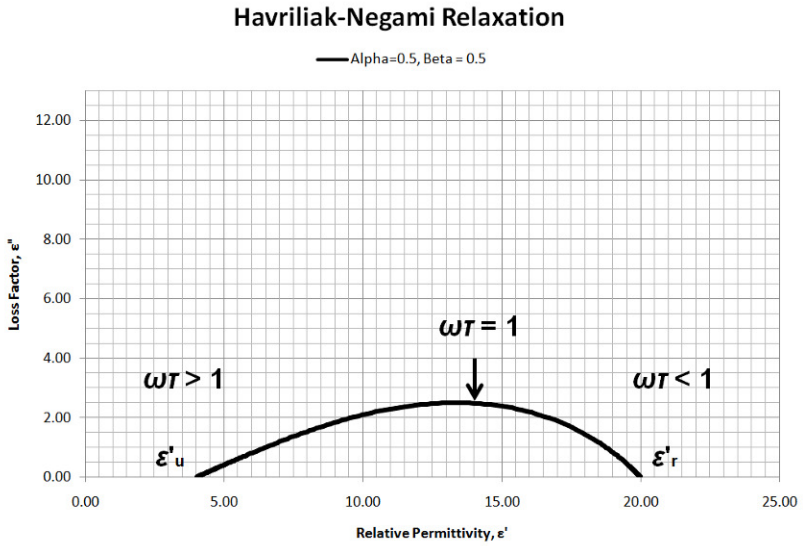

Figure 17-9
Cole-Cole plot of Havriliak-Negami relaxation

The Havriliak-Negami equation is simply a combination of the Cole-Cole and Cole-Davidson equations. If β = 1, then the result is Cole-Cole behavior. If α =1, then the result is Cole-Davidson behavior. If both α =1 and β = 1, then the Havriliak-Negami relaxation reduces to Debye relaxation.

The Havriliak-Negami relaxation of equation 17-31 may be factored into imaginary and real terms to yield expressions for loss factor and relative permittivity:

(eq. 17-32) $$\varepsilon'' = (\varepsilon'_r - \varepsilon'_u)\,(1 + 2(\omega\tau)^{\alpha}\cos(\pi\alpha/2) + (\omega\tau)^{2\alpha})^{-\beta/2}\sin(\beta\theta)$$

(eq. 17-33) $$\varepsilon' = \varepsilon'_u + (\varepsilon'_r - \varepsilon'_u)\,(1 + 2(\omega\tau)^{\alpha}\cos(\pi\alpha/2) + (\omega\tau)^{2\alpha})^{-\beta/2}\cos(\beta\theta)$$

Where:

(eq. 17-34) $$\theta = \tan^{-1}[(\omega\tau)^{\alpha}\sin(\pi\alpha/2) / (1 + (\omega\tau)^{\alpha}\cos(\pi\alpha/2))]$$

α = Empirical "broadness" parameter
β = Empirical "asymmetry" parameter
ε'_u = Unrelaxed (high frequency) relative permittivity
ε'_r = Relaxed (low frequency) relative permittivity
ω = $2\pi f$ (radians/s)
τ = Dipole relaxation time (s)

Contribution of ionic conduction to loss factor

Pure dielectric materials show only the Debye-type dipolar relaxation behavior; however, in reality almost all materials have some ionic content or impurity. The presence of mobile ions adds an ionic conduction term to loss factor, as seen in equation 17-21, repeated below:

(eq. 17-21) $$\varepsilon''_{MUT} = \sigma_{ion}/\omega\varepsilon_0 + (\varepsilon'_r - \varepsilon'_u)\frac{\omega\tau}{1 + (\omega\tau)^2}$$

In the case of equation 17-21, dipole relaxation is expressed with the Debye equation. More generally, loss factor may be expressed as the sum of ionic and dipolar loss factors, which is plotted in Figure 17-10:

(eq. 17-35) $$\varepsilon''_{MUT} = \varepsilon''_{ion} + \varepsilon''_{dipole}$$

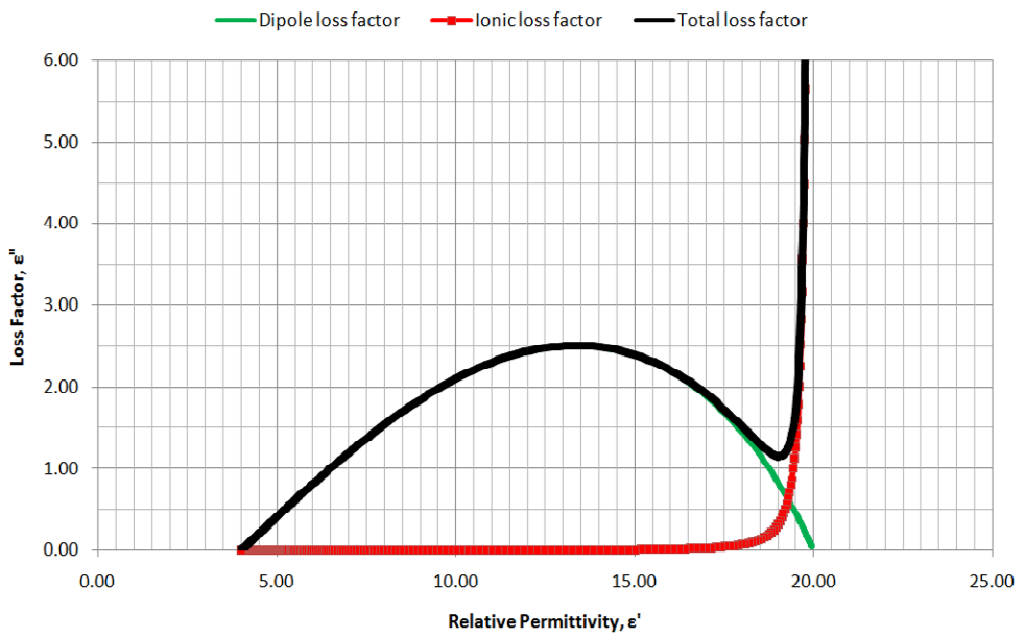

Figure 17-10
Addition of ionic and dipolar loss factors

Alternatively, the total loss factor is the sum of terms with frequency independent conductivity (σ_{DC}) and frequency dependent conductivity (σ_{AC}):

(eq. 17-36) $$\varepsilon''_{MUT} = (\sigma_{DC} + \sigma_{AC})/\omega\varepsilon_0$$

Where: $$\sigma_{DC} = \sigma_{ion}$$

$$\sigma_{AC} = \varepsilon_0 (\varepsilon'_r - \varepsilon'_u) \frac{\omega^2 \tau}{1 + (\omega\tau)^2}$$

As ionic conductivity increases, the effect on a Cole-Cole plot is shown in Figure 17-11:

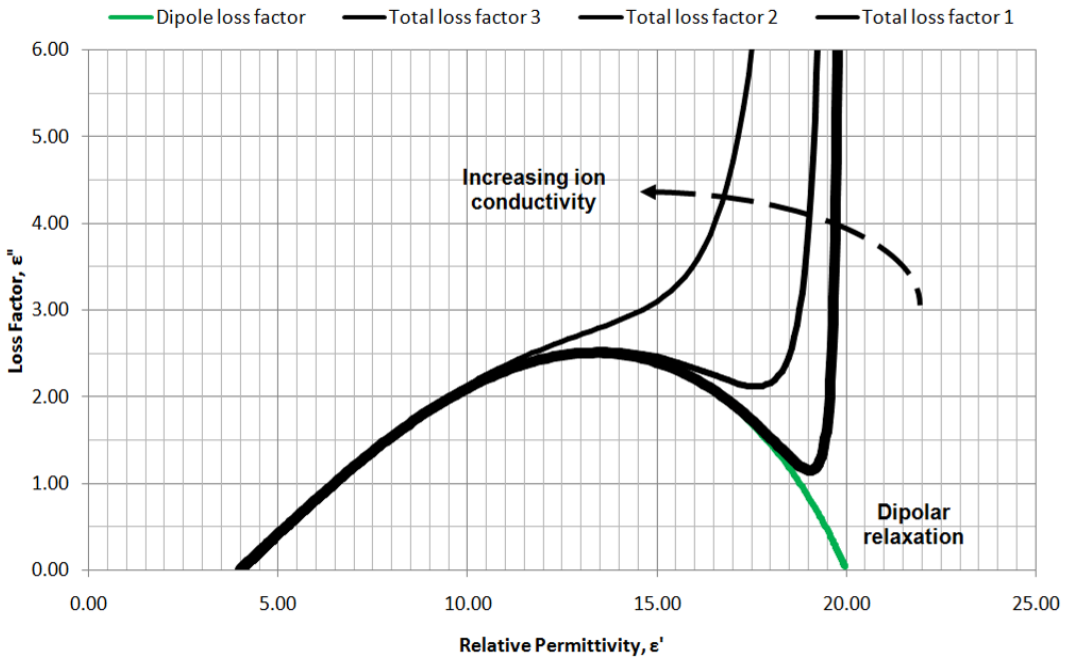

Figure 17-11
Total loss factor as a function of increasing ionic conductivity

When loss factor is plotted as a function of frequency, it is easier to see the relative contributions from ionic conductivity and dipolar relaxation. Dielectric measurements measure total loss factor, and information from a single frequency cannot separate the effects of ions and dipoles. If conductivity is sufficiently low, however, a frequency sweep can reveal the dipole loss peak, as shown in Figure 17-12 for low and intermediate conductivities. Note that high conductivity in Figure 17-12 has hidden the dipole peak.

As these plots illustrate, loss factor due to ions always dominates the response at sufficiently low frequencies. Dielectric cure monitoring takes advantage of this behavior to measure ionic conductivity without the influence of dipoles. The amount of crosslinking in a polymer or thermoset determines free ion mobility and therefore electrical conductivity. The amount of crosslinking also determines viscosity up to the gel point and modulus after the gel point. As a result, measurements of frequency independent conductivity σ_{DC} can probe the cure state of a material. Uniquely, dielectric measurements can observe the state of cure in-situ and in real time.

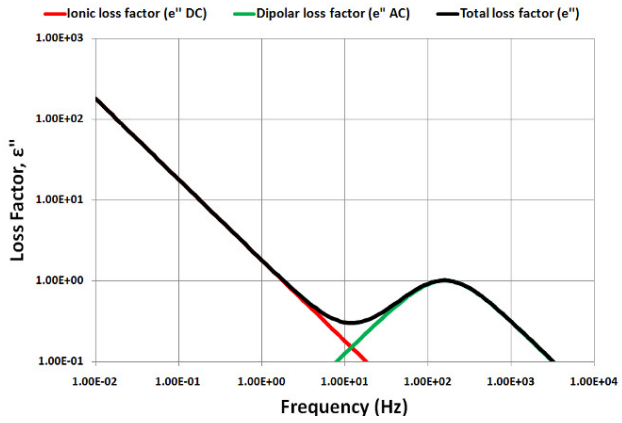

Low conductivity

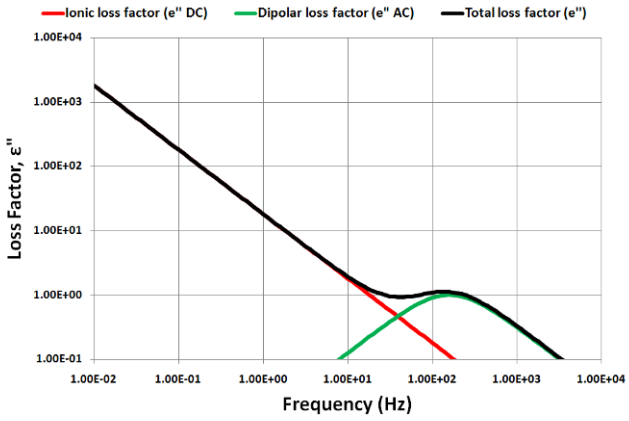

Intermediate conductivity

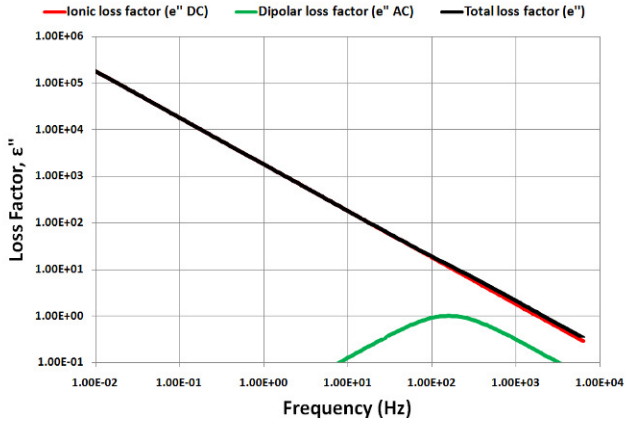

High conductivity

Figure 17-12
Effect of low, intermediate and high conductivity on loss factor (modeled)

Electrode polarization and the low frequency response of boundary layers

The presence of mobile ions in a polymer does not affect how its dipoles rotate. Therefore the frequency response of relative permittivity should not depend on the amount of ionic conductivity. Figure 17-13 shows this ideal behavior for relative permittivity—which is the same at low, intermediate and high conductivities—for the example modeled in Figure 17-12.

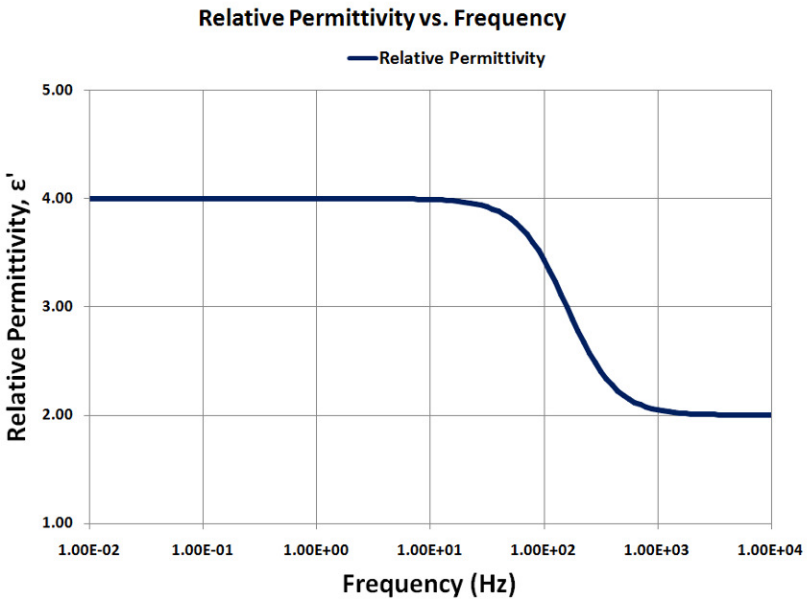

Figure 17-13
Ideal frequency response of relative permittivity
(Corresponding to example modeled in Figure 17-12)

Actual dielectric measurements of polymers usually reveal very large increases in permittivity at low frequencies or high conductivities. This behavior differs significantly from the Debye response and is *not* caused by a true change in permittivity. Instead, it is the result of an interaction between the material and the electrodes used to make measurements.

When a polymer has very high loss factor, ions accumulate at the electrode, where they are not exchanged because of an electrically insulating layer, such as a film or oxide or electrochemical potential barrier. This phenomenon is called *electrode polarization.* A boundary layer forms, depleted of ions, and only the dipolar response remains. As a result, the boundary layer acts as a capacitor in series with the bulk material.

In the presence of electrode polarization, very high permittivities result from use of the model of Figure 17-4, which is incorrect for the situation. The correct model of Figure 17-14 and the corresponding circuit of Figure 17-15 must be used instead.

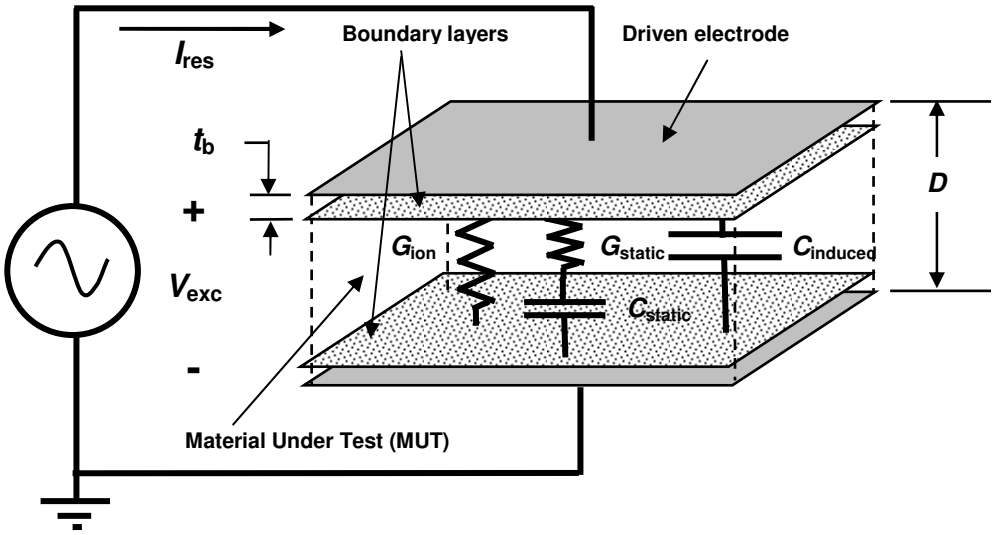

Figure 17-14
Boundary layer capacitances resulting from electrode polarization

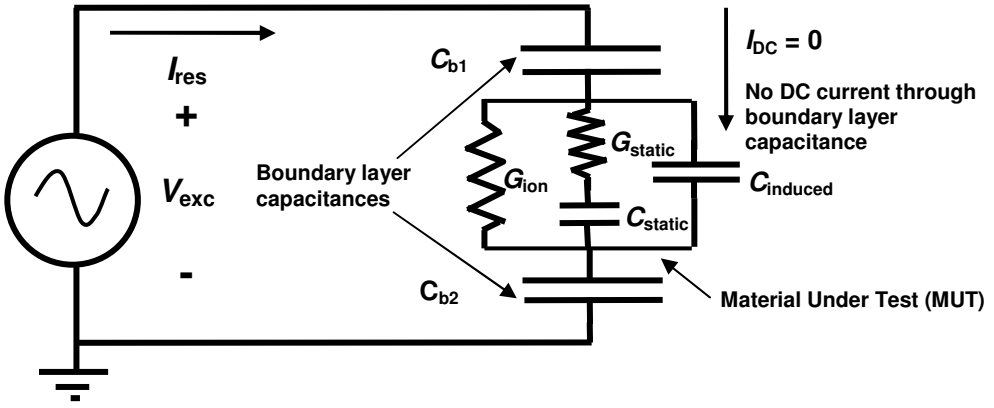

Figure 17-15
Circuit model of polymer with boundary layer capacitances

The boundary layer is very thin compared to the separation between electrodes. Consequently, boundary layer capacitance is much larger than bulk capacitance; it dominates the circuit response and acts as an open circuit to block DC current. Measurements of DC conductance are impossible in this case and the material appears primarily capacitive.

The low frequency electrical circuit of Figure 17-16 may be used to understand the resulting dielectric response. Here the two boundary layer capacitances, which are in series, have been combined into a single component with half the capacitance $C_b/2$. At low frequencies the admittances of capacitances due to static and induced dipoles are very low and only the conductive component G_{ion} contributes significantly to the response. This configuration is the same as the circuit representing the behavior of dipoles (G_{static} in series with C_{static} of Figure 17-4), and would have behavior similar to Debye relaxation.

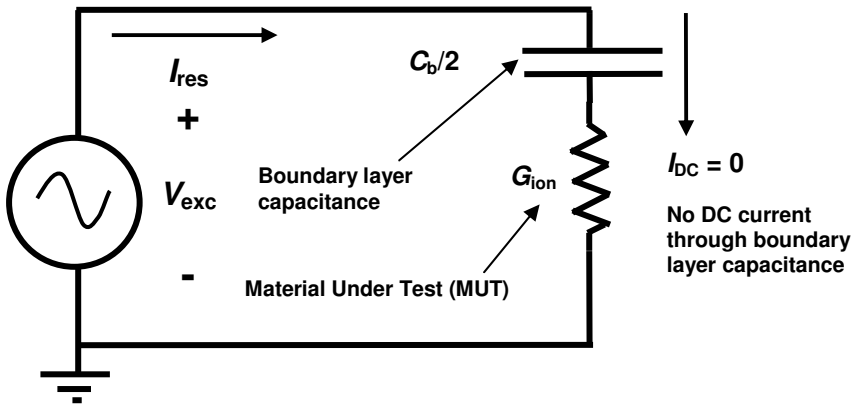

Figure 17-16
Low frequency circuit model with boundary layer capacitance

The uncorrected relative permittivity and loss factor resulting from electrode polarization are given by the following equations[5]:

(eq. 17-37) $$\varepsilon'_x = \varepsilon' (D / 2t_b) \frac{(\varepsilon''/\varepsilon')^2 + (D / 2t_b)}{(\varepsilon''/\varepsilon')^2 + (D / 2t_b)^2)}$$ Apparent relative permittivity

(eq. 17-38) $$\varepsilon''_x = \varepsilon'' (D / 2t_b) \frac{(D / 2t_b) - 1}{(\varepsilon''/\varepsilon')^2 + (D / 2t_b)^2)}$$ Apparent loss factor

Where: t_b = boundary layer thickness
D = distance between electrodes or plate separation
ε' = actual permittivity
ε'' = actual loss factor

At low loss factors (high frequencies or low conductivities), electrode polarization has little effect on either the measured permittivity or loss factor. At sufficiently high loss factors, however, the apparent permittivity begins to increase, causing loss factor on the Cole-Cole plot of Figure 17-17 to deviate from its ideal, vertical trajectory.

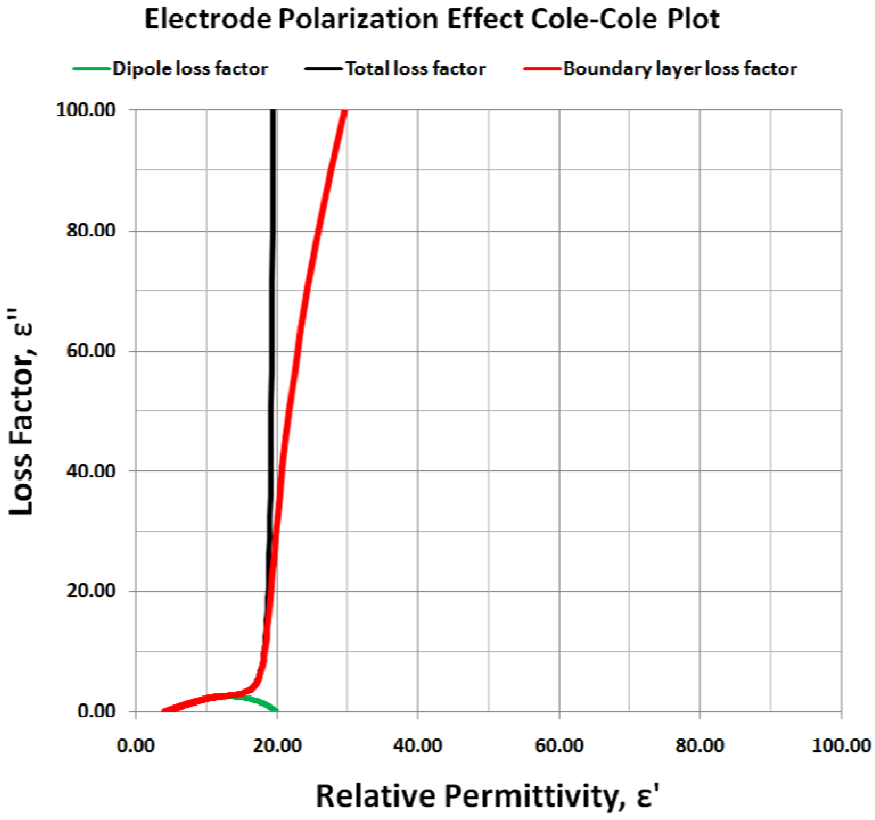

Figure 17-17
Deviation of Cole-Cole plot trajectory caused by electrode polarization

As the *true* material loss factor increases even further, the *apparent* permittivity continues to increase and at some point the *apparent* loss factor actually begins to decrease. The Cole-Cole plot becomes the arc of Figure 17-18. Eventually, when the true loss factor is high enough (i.e. frequency is sufficiently low or conductivity is sufficiently high), the apparent permittivity reaches a very high limit and the apparent loss factor approaches zero. The result is a semi-circle

on the Cole-Cole plot like that produced by the Debye relaxation, but with a much larger radius. This radius depends on the thickness of the boundary layer relative to the separation between electrodes.

Because of electrochemical potential barriers, electrode polarization almost always occurs. If the resulting boundary layer is very thin, the effect on loss factor is reduced, and the radius of the Cole-Cole plot is very large. While the change in apparent loss factor may be small, the change in apparent relative permittivity usually remains significant.

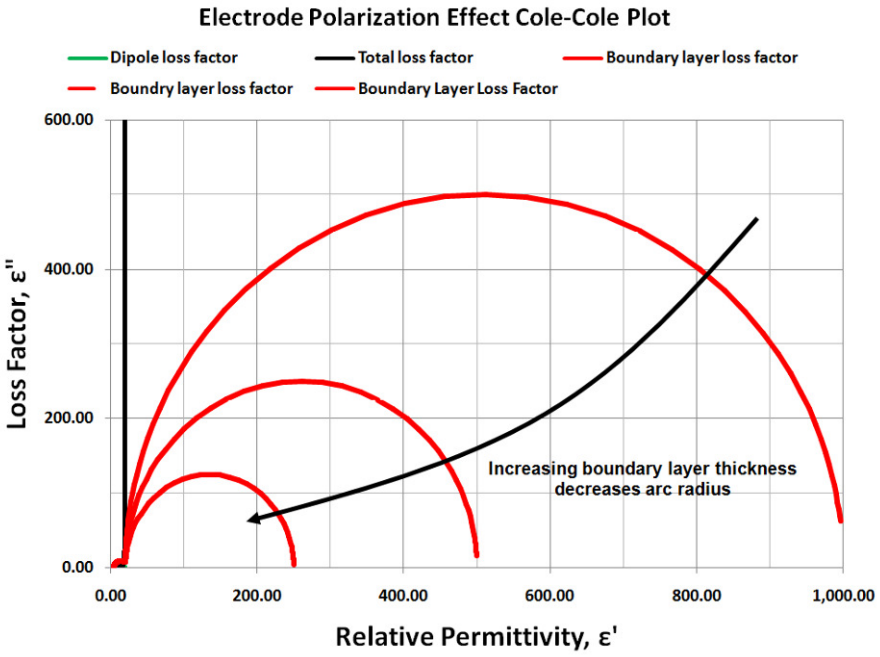

Figure 17-18
Cole-Cole plot trajectories caused by electrode polarization

Figure 17-19 compares the frequency response of true permittivity, which has a Debye-type relaxation, with the apparent permittivity resulting from a boundary layer. In this case the modeled behavior demonstrates how the relative relationship between the dipolar and the boundary layer time constants determines visibility of the dipole relaxation.

Under the same conditions modeled in Figure 17-19, Figure 17-20 compares the frequency response of true loss factor with the apparent loss factor resulting from a boundary layer. Note that the apparent loss factor has a peak of very high value at very low frequency, while true loss factor does not. In the past this artificial loss peak has been attributed to a large dipole relaxation.

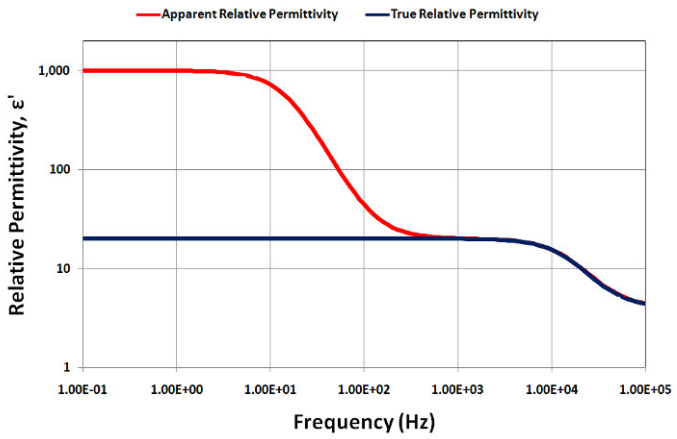

Small dipole time constant

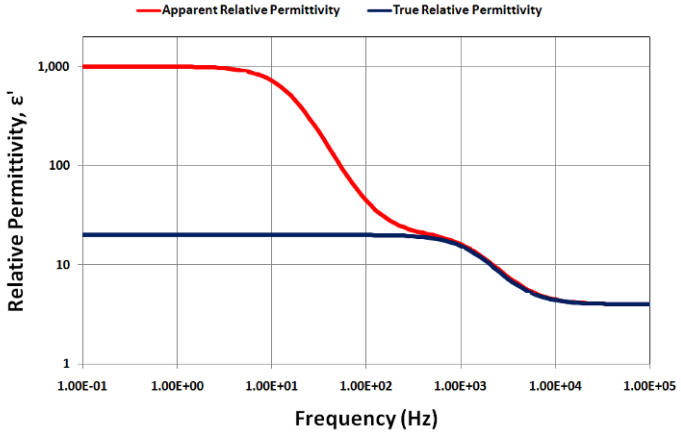

Intermediate dipole time constant

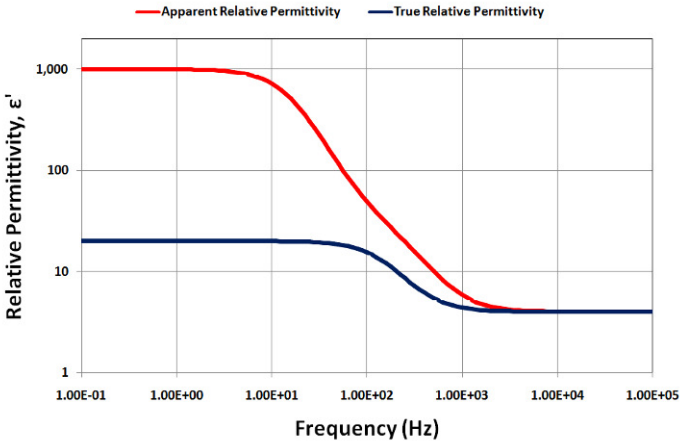

Large dipole time constant

Figure 17-19
Relative permittivity and the influence of electrode polarization

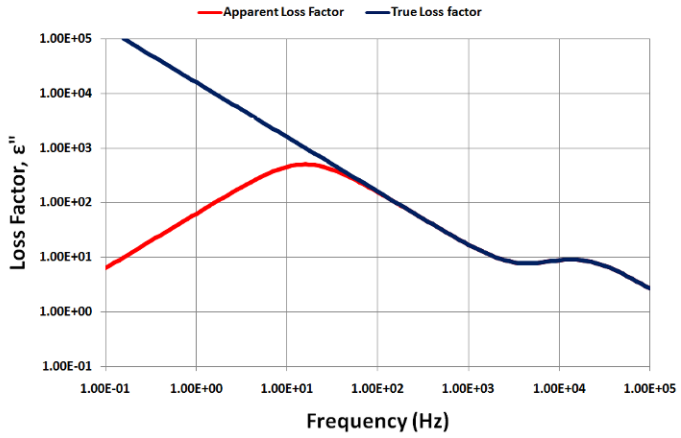

Small dipole time constant

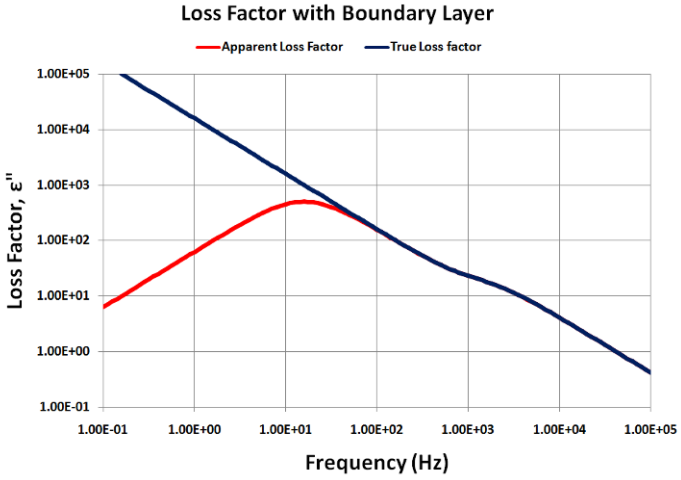

Intermediate dipole time constant

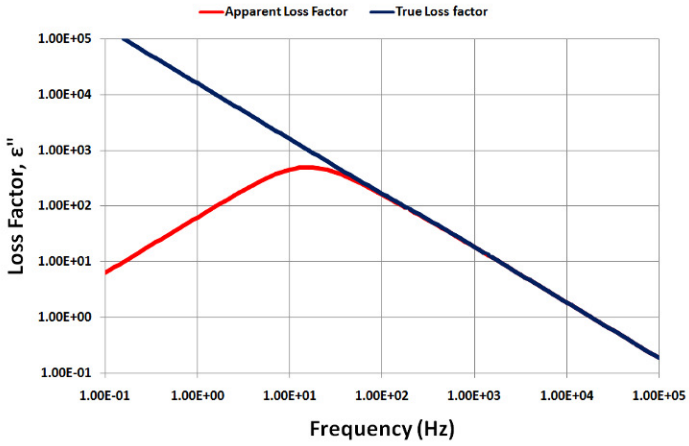

Large dipole time constant

Figure 17-20
Loss factor and the influence of electrode polarization

Dipole and boundary layer loss peaks

The differences between dipole and boundary layer loss peaks are:[6]

- Dipole loss peaks for most polymers are rarely greater than 3 and almost never greater than ~10
- Boundary layer loss peaks are usually greater than ~100
- Boundary layer loss peaks vary with electrode separation, while dipole loss peaks do not

Boundary layer effect on curing materials

Figures 17-21 and 17-22 show the effect of boundary layers on apparent dielectric properties during cure of "five-minute" epoxy. In this case, unlike for Figures 17-19 and 17-20, permittivity and loss factor are changing with time and temperature.

The curing reaction is exothermic and temperature increases at first, which causes viscosity to decrease. Consequently, both conductivity and loss factor increase during this initial period. After a certain time, temperature is high enough for the accelerating reaction rate to dominate—viscosity begins to increase because the amount of polymerization overcomes the decrease in viscosity due to temperature. At this point conductivity and loss factor also decrease.

After loss factor reaches its peak, it declines to approach a constant value at the end of cure. For frequencies of 10 Hz or greater, this peak in loss factor is well behaved. For 1 Hz, however, the boundary layer effect distorts loss factor by depressing the peak and creating two satellite peaks in its place. Before researchers understood electrode polarization in polymers, the second satellite peak was thought to coincide with gelation. In fact, these peaks are artifacts of an incorrect electrical model. Fortunately, in many cases it is possible to mathematically correct the distortion caused by boundary layers (See Application Note AN2.16, *Electrode Polarization and Boundary Layer Effects*).

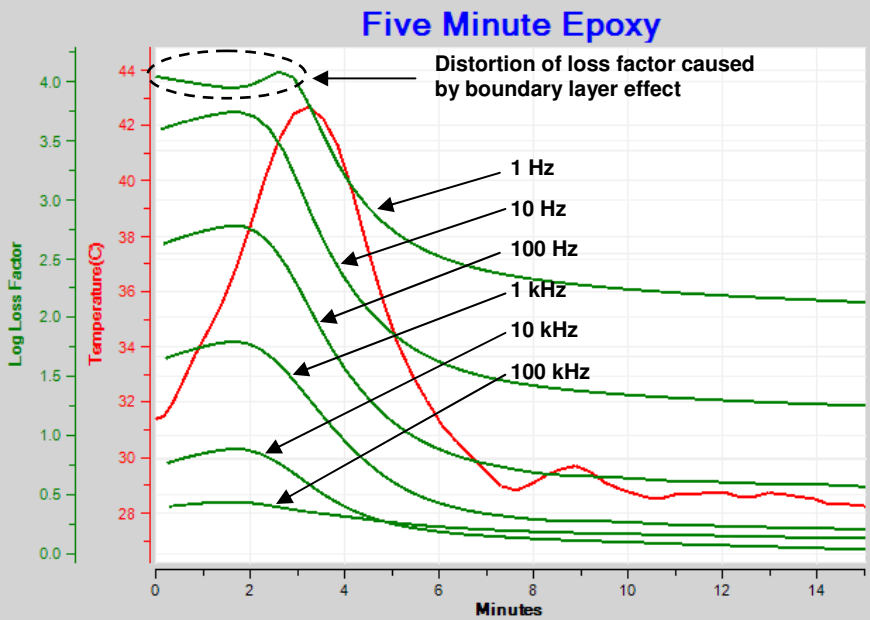

Figure 17-21
Loss factor of curing epoxy, showing effect of boundary layer

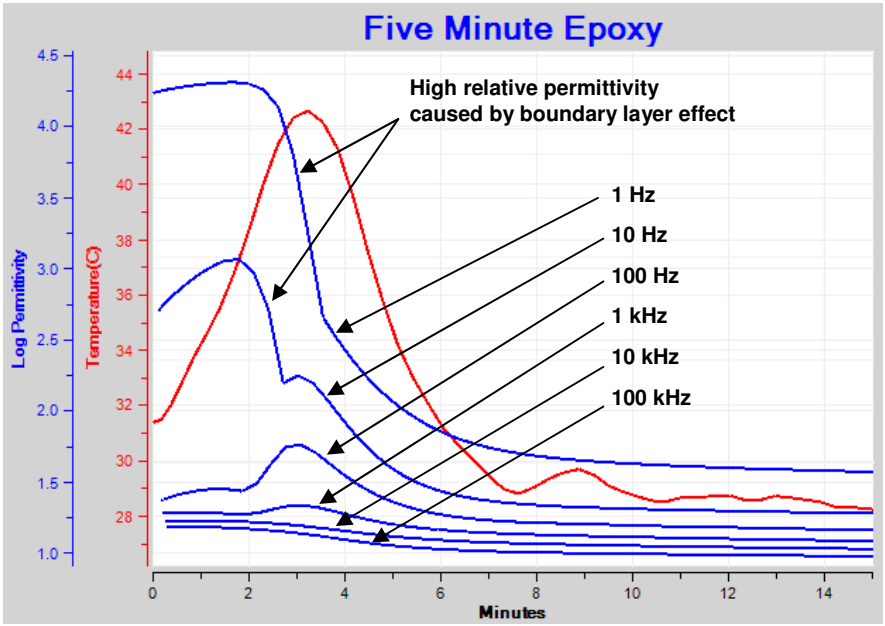

Figure 17-22
Relative permittivity of curing epoxy, showing effect of boundary layer

For this epoxy, relative permittivity has a clear Debye-type relaxation visible at 100 kHz and 10 kHz. At 1 kHz and 100 Hz, relative permittivity displays a peak, which is caused by the temperature response of permittivity. Note that maximum permittivity coincides with the maximum temperature of this test. At

10 Hz the boundary layer effect artificially increases apparent permittivity and partially hides this peak in permittivity. Finally, at 1 Hz the boundary layer dominates completely and relative permittivity exceeds 10,000 at its maximum—a completely unrealistic value.

Inhomogeneities and Maxwell-Wagner-Sillars polarization

Until now this application note has discussed only homogeneous polymers. The electrical response, however, is not as straightforward with multi-layer films, fiberglass composites or materials with several phases. The Maxwell-Wagner-Sillars[7,8] effect (sometimes simply called the Maxwell-Wagner effect) describes dielectric behavior resulting from charge accumulation at the boundaries of inhomogeneities. The Maxwell-Wagner-Sillars model uses small spheres embedded in an infinite dielectric as shown in Figure 17-23. In essence, Maxwell-Wagner-Sillars polarization is the same as electrode polarization, resulting in a large parasitic capacitance in series with bulk material.

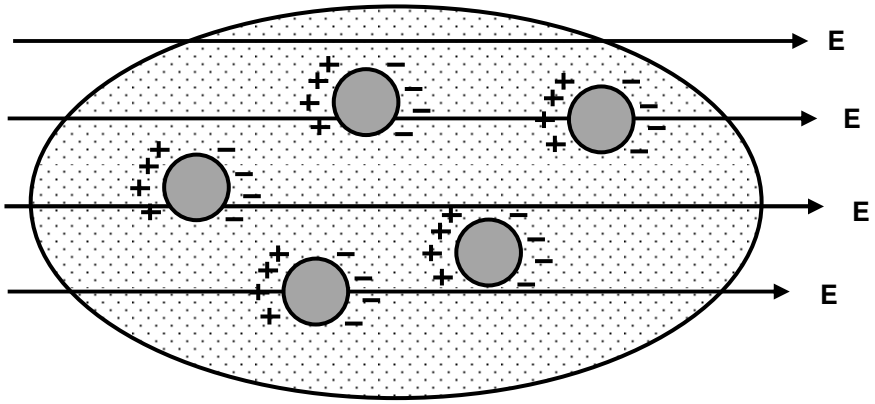

Figure 17-23
Maxwell-Wagner-Sillars polarization

This model has a dielectric response like that of a boundary layer, with very high *apparent* permittivities and distortions in *apparent* loss factor. Depending on the nature of the inhomogeniety, the Maxwell-Wagner-Sillars effect can become very complicated. In the case of multi-layer films, the dielectric behavior can be identical to that of a boundary layer because the geometries are the same.

Some analysis of insulating fibers in a conductive material has attempted to simulate the cure of fiberglass or Kevlar epoxy composites. For reasonable fiber geometries, permittivity is affected but loss factor is not, which agrees with

experimental evidence.[6] In some cases loss factor increases, possibility because of an increase in ion concentration from the fibers.

Summary of the electrical model of polymers

- Induced dipole rotation
  - Modeled by $C_{induced}$, bulk capacitance from induced dipoles on nonpolar bonds
  - Frequency independent response
- Static dipole rotation
  - Modeled by C_{static} in series with G_{static}, capacitance and conductance from molecular dipoles
  - Frequency dependent response
  - Cole-Cole plot is an arc between relaxed and unrelaxed permittivity limits
  - Dipole loss factor peaks rarely greater than 3 and almost never greater than ~10
- Ionic conduction
  - Modeled by G_{ion}, bulk conductance from mobile ions
  - Frequency independent response
  - Cole-Cole plot is a vertical line
- Electrode polarization
  - Modeled by C_b, boundary layer capacitance on electrodes
  - Frequency dependent response in combination with G_{ion}
  - Cole-Cole plot is an arc over unrealistically large permittivities
  - Boundary layer loss factor peaks usually greater than ~100
- Maxwell-Wagner-Sillars polarization
  - Modeled by spheres in a dielectric material
  - Frequency dependent response in combination with G_{ion}
  - Cole-Cole plot similar to result from electrode polarization

References

1. Cole, K.S.; Cole, R.H., "Dispersion and Absorption in Dielectrics - I Alternating Current Characteristics". *Journal of Chemical Physics,* **9**: 341–352 (1941).

2. Cole, K.S.; Cole, R.H., "Dispersion and Absorption in Dielectrics - II Direct Current Characteristics". *Journal of Chemical Physics,* **10**: 98–105 (1942).

3. Davidson, D.W. and Cole, R.H., "Dielectric relaxation in glycerol, propylene glycol, and normal-propanol". *Journal of Chemical Physics*, 19(12):1484–1490 (1951).

4. Havriliak, S.; Negami, S., "A complex plane representation of dielectric and mechanical relaxation processes in some polymers". *Polymer*, **8**:161-210 (1967).

5. Day, D.R.; Lewis J.; Lee, H.L. and Senturia, S.D., *Journal of Adhesion*, V18, p.73 (1985).

6. Day, D.R., *Dielectric Properties of Polymeric Materials*, Micromet Instruments, (1988).

7. Wagner, K.W., *Arch. Elektrotech*. 2:378 (1914).

8. Sillars, R.W., *J. Inst. Elm. Engrs* (London) 80:378 (1937).

Lambient Technologies LLC
649 Massachusetts Avenue, Cambridge, MA 02139
857-242-3963
www.lambient.com
info@lambient.com

